PERGAMON

International Journal of Solids and Structures 37 (2000) 435–459

INTERNATIONAL JOURNAL OF SOLIDS and STRUCTURES

www.elsevier.com/locate/ijsolstr

Iterative free-edge stress analysis of composite laminates under extension, bending, twisting and thermal loadings

Maenghyo Cho*, Heung Soo Kim

Department of Aerospace Engineering, Inha University, 253 Yong-Hyun Dong, Nam-Ku, Inchon 402-751, South Korea

Received 14 July 1998; in revised form 6 January 1999

Abstract

An iterative method has been applied to analyze free edge interlaminar stresses of composite laminates which are subject to extension, bending, twisting and thermal loads. The stresses, which satisfy the traction-free conditions not only at the free edges but also at the top and bottom surfaces of laminates, are obtained by using the complementary virtual work and the extended Kantorovich method. In order to obtain accurate interlaminar stresses, static and kinematic continuity conditions are applied at the interfaces between plies through iterations. To demonstrate the validity of the proposed method, cross-ply, angle-ply, and quasi-isotropic laminates are considered. Through the iteration processes, the convergence of the solutions is demonstrated. The present method provides accurate stresses in the interior and near the free edges of laminates. It can be utilized as an analytical tool to predict interlaminar stresses under the loads of mechanical and thermal combined.

Keywords: Interlaminar stresses; Free edge; Composite laminates; Complementary energy principle

1. Introduction

Numerous research efforts have been made to resolve serious stress concentration/singularity near the free edges of composite laminates which are caused by dissimilar material properties between plies. However, since the difficulties occur during the process of obtaining the exact singular elasticity solutions of free-edge interlaminar stress problems, approximate methods have been pursued which are based on numerical or analytical approaches. Although recently developed numerical methods consist of either finite element methods or boundary integral methods, simple and accurate analytical methods are preferred in the preliminary design stage since they facilitate parametric study.

* Corresponding author.
E-mail address: mhcho@dragon.inha.ac.kr (M. Cho)

0020-7683/00/$ - see front matter
PII: S0020-7683(99)00014-1

After Spilker and Chou (1980) demonstrated the importance of satisfying the traction-free conditions at the edges, stress-based methods have been proposed. These methods divide stress functions into in-plane and out-of-plane functions. With appropriate stress function assumptions, the interlaminar stresses at free edges have been calculated. Kassapoglou and Lagace (1986) determined the stresses based on the integrated form of the force and moment equilibriums. However, at free edges the results do not satisfy the pointwise traction-free conditions through the thickness. Thus its accuracy of predicted stresses in out-of-plane direction is not reliable. Yin (1994a, 1994b) used piecewise polynomial approximations for the out-of-plane stress functions which are continuous over each layer, and the interlaminar stresses which are also continuous at the layer interfaces. His solution satisfies the free edge boundary conditions in a pointwise sense.

Recently, Flanagan (1994) proposed an alternative efficient method in which the out-of-plane stress functions were assumed to be the solutions of the free vibration of a clamped–clamped beam. Also, using the principle of complementary minimum energy, a simple method was proposed to determine the in-plane stress functions. The stress functions given by his approach did not satisfy displacement continuity conditions at the ply interfaces. Thus, the out-of-plane stress distributions were not predicted accurately, and oscillations appeared. In addition, his results could not recover the classical lamination theory (CLT) solution in the interior of laminates.

To accurately determine interlaminar stresses, stresses should be zero at the free edges and the top/bottom surfaces of composite plates, while at the ply interfaces the stresses and displacements should be continuous. The extended Kantorovich method has been applied by Cho and Yoon (1997) to efficiently predict approximate interlaminar stresses at the straight free edges of laminates under the extension loads.

Analysis of free-edge stresses under bending or twisting are less common than of those under extension loads. However, the importance of bending and twisting cases can not be neglected in the least. In the present study, the iterative method is extended to the problems under the extension, bending, twisting and thermal loads to provide accurate interlaminar stress distributions near the free edges.

2. Formulation

The geometry of composite laminate with free edges is given in Fig. 1. The laminate consists of orthotropic materials. The thickness of each ply is all same, and the plies have arbitrary angles relative to the x axis. Extension, bending, twisting and thermal residual stresses are considered.

The linear elastic constitutive equations are assumed in each ply and they are expressed in the following form:

$$\begin{Bmatrix} \epsilon_1 \\ \epsilon_2 \\ \epsilon_3 \\ \epsilon_4 \\ \epsilon_5 \\ \epsilon_6 \end{Bmatrix} = \begin{bmatrix} S_{11} & S_{12} & S_{13} & 0 & 0 & S_{16} \\ S_{12} & S_{22} & S_{23} & 0 & 0 & S_{26} \\ S_{13} & S_{23} & S_{33} & 0 & 0 & S_{36} \\ 0 & 0 & 0 & S_{44} & S_{45} & 0 \\ 0 & 0 & 0 & S_{45} & S_{55} & 0 \\ S_{16} & S_{26} & S_{36} & 0 & 0 & S_{66} \end{bmatrix} \begin{Bmatrix} \sigma_1 \\ \sigma_2 \\ \sigma_3 \\ \sigma_4 \\ \sigma_5 \\ \sigma_6 \end{Bmatrix} + \begin{bmatrix} \alpha_1 \\ \alpha_2 \\ \alpha_3 \\ 0 \\ 0 \\ \alpha_6 \end{bmatrix} \Delta T, \tag{1}$$

From the first row of Eq. (1), the following relationship is obtained

$$\sigma_1 = \frac{(\epsilon_1 - \alpha_1 \Delta T - S_{ij}\sigma_j)}{S_{11}} \ (j = 2,3,6). \tag{2}$$

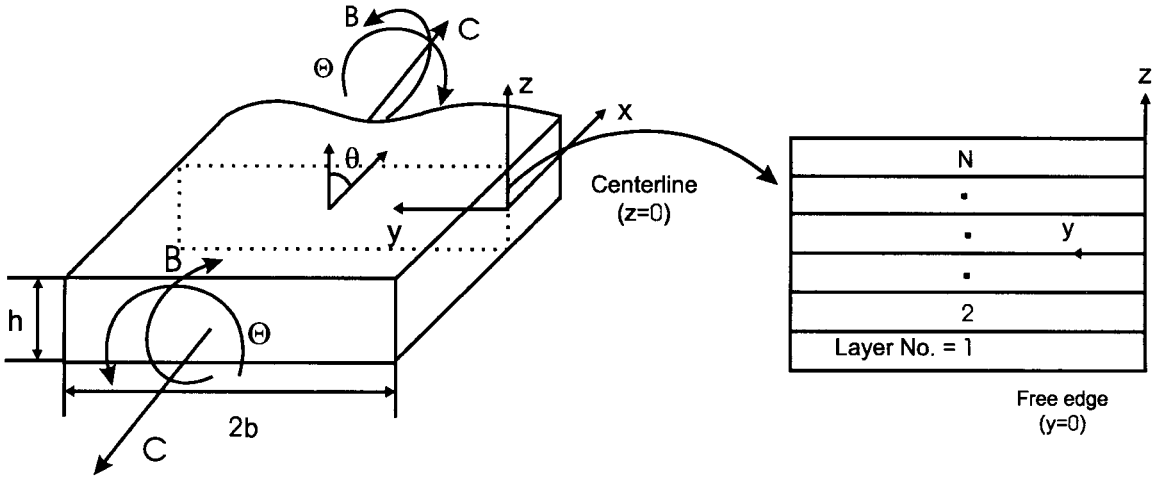

Fig. 1. Geometry of composite laminate with free edges.

Substituting Eq. (2) into Eq. (1), all the strains can be expressed as

$$\epsilon_i = \hat{S}_{ij}\sigma_j + \frac{S_{i1}}{S_{11}}\epsilon_1 + \hat{\alpha}_i \Delta T \ (i,j = 2,3,\ldots,6), \tag{3}$$

where

$$\hat{S}_{ij} = S_{ij} - \frac{S_{1i}S_{1j}}{S_{11}}, \quad \hat{\alpha}_i = \alpha_i - \frac{\alpha_1 S_{i1}}{S_{11}}. \tag{4}$$

For the given geometric configuration of laminates, the boundary conditions at the free edge and the surfaces of the top and bottom faces are given in Eq. (5).

$$\sigma_2 = \sigma_4 = \sigma_6 = 0 \text{ at } y = 0,b$$

$$\sigma_3 = \sigma_4 = \sigma_5 = 0 \text{ at } z = \pm h/2. \tag{5}$$

Generalized plane strain states are assumed and the stress fields are independent of the x-axis.

$$u(x,y,z) = (Ay - Bz + C)x + U(y,z) + \omega_1 z - \omega_2 y + u_0,$$

$$v(x,y,z) = -A\frac{x^2}{2} - \Theta xz + V(y,z) + \omega_2 x - \omega_3 z + v_0$$

$$w(x,y,z) = B\frac{x^2}{2} + \Theta xy + W(y,z) + \omega_3 y - \omega_1 x + w_0, \tag{6}$$

where A and B characterize the bending of the body in the x–z and x–y plane, respectively, C characterizes the extension of the body about the x-axis. Θ is the relative angle of rotation about the x-axis. The constants ω_1, ω_2, ω_3, u_0, v_0, w_0 characterize rigid displacements of the body. The coordinates are nondimensionalized, as follows:

$$\eta = z/h,\ \xi = y/h. \tag{7}$$

Following the previous work of Yin (1994a, 1994b), the present analysis adopts the stress function approach and uses the complementary virtual work principle. Lekhnitskii (1963) stress functions are introduced to satisfy pointwise equilibrium equations automatically. These stress functions can be divided into the in-plane and out-of-plane functions,

$$\frac{\partial^2 F}{\partial \eta^2} = \sigma_2, \quad \frac{\partial^2 F}{\partial \xi^2} = \sigma_3, \quad \frac{\partial^2 F}{\partial \eta \partial \xi} = -\sigma_4$$

$$\frac{\partial \Psi}{\partial \xi} = -\sigma_5, \quad \frac{\partial \Psi}{\partial \eta} = \sigma_6, \tag{8}$$

where

$$F = \sum_{i=1}^{n} f_i(\xi) g_i(\eta), \quad \Psi = \sum_{i=1}^{n} p_i(\xi) g_i^I(\eta) \tag{9}$$

for extension, bending and thermal loadings (Case I). The superscript I in Eq. (9) denotes differentiation with respect to η.

$$F = \sum_{i=1}^{n} f_i(\xi) g_i(\eta), \quad \Psi = \sum_{i=1}^{n} p_i(\xi) h_i(\eta) \tag{10}$$

for twisting load (Case II).

The governing equations are obtained by taking the principle of complementary virtual work:

$$0 = \int\int\int u_i \delta\sigma_{ij,j}\, \mathrm{d}x\, \mathrm{d}y\, \mathrm{d}z = \int\int\int \{(u_i \delta\sigma_{ij})_{,j} - u_{i,j}\delta\sigma_{ij}\}\mathrm{d}x\, \mathrm{d}y\, \mathrm{d}z$$

$$= \int\int_S u_i \delta\sigma_{ij} n_j\, \mathrm{d}A - \int\int\int \frac{1}{2}(u_{i,j} + u_{j,i})\delta\sigma_{ij}\, \mathrm{d}x\, \mathrm{d}y\, \mathrm{d}z. \tag{11}$$

By using traction-free boundary conditions and neglecting rigid body motions, one obtains

$$\int\int (\Delta u \delta\sigma_{xx} + \Delta v \delta\sigma_{yx} + \Delta w \delta\sigma_{zx})\mathrm{d}y\, \mathrm{d}z = \int\int \epsilon_{ij}\delta\sigma_{ij}\, \mathrm{d}y\, \mathrm{d}z, \tag{12}$$

where

$$\Delta u = C - Bz, \quad \Delta v = -\Theta z, \quad \Delta w = \frac{B}{2} + \Theta y. \tag{13}$$

2.1. 1st process: calculation of in-plane stress functions from an initial assumption

The in-plane stress functions are determined from the initially assumed basis set of out-of-plane stress functions. The out-of-plane functions must satisfy traction-free conditions at the top and bottom surfaces (i.e. The stress functions and their first derivatives have to be zero in those regions). The out-of-plane functions are assumed to be the eigenmodes of a clamped-clamped beam and a simply-supported beam. The stress functions $g_i(\eta)$ and $h_i(\eta)$ through the thickness are given as follows. The even function

set is expressed as:

$$g_i(\eta) = \cos(k_i\eta) + \sigma_i \cosh(k_i\eta), \tag{14}$$

where the k_i's are the solutions of the following characteristic equations,

$$\cosh(k_i/2)\sin(k_i/2) + \cos(k_i/2)\sinh(k_i/2) = 0$$

and

$$\sigma_i = -\frac{\cos(k_i/2)}{\cosh(k_i/2)} \tag{15}$$

The odd function set is expressed as:

$$g_i(\eta) = \sin(k_i\eta) + \sigma_i \sinh(k_i\eta), \tag{16}$$

where the k_i's are the solutions of following characteristic equations,

$$\cosh(k_i/2)\sin(k_i/2) - \cos(k_i/2)\sinh(k_i/2) = 0$$

$$\sigma_i = -\frac{\cos(k_i/2)}{\cosh(k_i/2)} \tag{17}$$

and

$$h_i(\eta) = \sin\left(i\pi\eta + \frac{i\pi}{2}\right). \tag{18}$$

Substituting Eq. (8) into Eq. (12), the stresses are expressed in terms of f_i and p_i. Eq. (12) can be expressed as follows, after integration by parts.

$$\int\left[a_{ij}^{(4)} f_j^{\mathrm{IV}} + a_{ij}^{(2)} f_j^{\mathrm{II}} + a_{ij}^{(0)} f_j + b_{ij}^{(2)} p_j^{\mathrm{II}} + b_{ij}^{(0)} p_j + r_i\right]\delta f_i \,\mathrm{d}\xi + \int\left[c_{ij}^{(2)} p_j^{\mathrm{II}} + c_{ij}^{(0)} p_j + d_{ij}^{(2)} f_j^{\mathrm{II}} + d_{ij}^{(0)} f_j + s_i\right]\delta$$

$$p_i \,\mathrm{d}\xi = 0, \quad (i,j = 1,2,\ldots,n) \tag{19}$$

where, for Case I,

$$a_{ij}^{(4)} = \int \hat{S}_{33} g_i g_j \,\mathrm{d}\eta,$$

$$a_{ij}^{(2)} = \int \hat{S}_{23}\left(g_i^{\mathrm{II}} g_j + g_i g_j^{\mathrm{II}}\right)\mathrm{d}\eta - \int \hat{S}_{44} g_i^{\mathrm{I}} g_j^{\mathrm{I}} \,\mathrm{d}\eta,$$

$$a_{ij}^{(0)} = \int \hat{S}_{22} g_i^{\mathrm{II}} g_j^{\mathrm{II}} \,\mathrm{d}\eta,$$

$$b_{ij}^{(2)} = \int \hat{S}_{36} g_i g_j^{\mathrm{II}} \,\mathrm{d}\eta - \int \hat{S}_{45} g_i^{\mathrm{I}} g_j^{\mathrm{I}} \,\mathrm{d}\eta,$$

$$b_{ij}^{(0)} = \int \hat{S}_{26} g_i^{\mathrm{II}} g_j^{\mathrm{II}} \, \mathrm{d}\eta,$$

$$c_{ij}^{(2)} = -\int \hat{S}_{55} g_i^{\mathrm{I}} g_j^{\mathrm{I}} \, \mathrm{d}\eta,$$

$$c_{ij}^{(0)} = \int \hat{S}_{66} g_i^{\mathrm{II}} g_j^{\mathrm{II}} \, \mathrm{d}\eta,$$

$$d_{ij}^{(2)} = \int \hat{S}_{36} g_i^{\mathrm{II}} g_j \, \mathrm{d}\eta - \int \hat{S}_{45} g_i^{\mathrm{I}} g_j^{\mathrm{I}} \, \mathrm{d}\eta,$$

$$d_{ij}^{(0)} = \int \hat{S}_{26} g_i^{\mathrm{II}} g_j^{\mathrm{II}} \, \mathrm{d}\eta,$$

$$r_i = \int \left[\frac{S_{12}}{S_{11}} (C - Bh\eta) + \hat{\alpha}_2 \Delta T \right] g_i^{\mathrm{II}} \, \mathrm{d}\eta,$$

$$s_i = \int \left[\frac{S_{16}}{S_{11}} (C - Bh\eta) + \hat{\alpha}_6 \Delta T \right] g_i^{\mathrm{II}} \, \mathrm{d}\eta \tag{20}$$

and, for Case II,

$$a_{ij}^{(4)} = \int \hat{S}_{33} g_i g_j \, \mathrm{d}\eta,$$

$$a_{ij}^{(2)} = \int \hat{S}_{23} \left(g_i^{\mathrm{II}} g_j + g_i g_j^{\mathrm{II}} \right) \mathrm{d}\eta - \int \hat{S}_{44} h_i g_j^{\mathrm{I}} \, \mathrm{d}\eta,$$

$$a_{ij}^{(0)} = \int \hat{S}_{22} g_i^{\mathrm{II}} g_j^{\mathrm{II}} \, \mathrm{d}\eta,$$

$$b_{ij}^{(2)} = \int \hat{S}_{36} g_i h_j^{\mathrm{I}} \, \mathrm{d}\eta - \int \hat{S}_{45} g_i^{\mathrm{I}} h_j \, \mathrm{d}\eta,$$

$$b_{ij}^{(0)} = \int \hat{S}_{26} g_i^{\mathrm{II}} h_j^{\mathrm{I}} \, \mathrm{d}\eta,$$

$$c_{ij}^{(2)} = -\int \hat{S}_{55} h_i h_j \, \mathrm{d}\eta,$$

$$c_{ij}^{(0)} = \int \hat{S}_{66} h_i^{\mathrm{I}} h_j^{\mathrm{I}} \, \mathrm{d}\eta,$$

$$d_{ij}^{(2)} = \int \hat{S}_{36} h_i^{\mathrm{I}} g_j \, \mathrm{d}\eta - \int \hat{S}_{45} h_i g_j^{\mathrm{I}} \, \mathrm{d}\eta,$$

$$d_j^{(0)} = \int \hat{S}_{26} h_i^{\mathrm{I}} g_j^{\mathrm{II}} \, \mathrm{d}\eta,$$

$$r_i = 0,$$

$$s_i = -\int 2\Theta h h_i \, \mathrm{d}\eta. \tag{21}$$

The boundary terms, induced by integration by parts, are eliminated from the free edge conditions $\sigma_2 = \sigma_4 = \sigma_6 = 0$.

In Eq. (19), the governing equations are reduced to the ordinary differential equations where $f_i(\xi)$ and $p_i(\xi)$ are coupled. The homogeneous solutions of f_i and p_i are assumed to be of the following forms,

$$f_i = v_i^f e^{\lambda\xi}, \quad p_i = v_i^p e^{\lambda\xi} \tag{22}$$

Substituting Eq. (21) into Eq. (19), the ordinary differential equations are reduced to the following:

$$a_{ij}^{(0)} v_j^f + \left(a_{ij}^{(2)} + \lambda^2 a_{ij}^{(4)}\right) v_j^{f^{\mathrm{II}}} + \left(b_{ij}^{(0)} + \lambda^2 b_{ij}^{(2)}\right) v_j^p = 0,$$

$$d_{ij}^{(0)} v_j^f + d_{ij}^{(2)} v_j^{f^{\mathrm{II}}} + \left(c_{ij}^{(0)} + \lambda^2 c_{ij}^{(2)}\right) v_j^p = 0,$$

$$\lambda^2 v_j^f - v_j^{f^{\mathrm{II}}} = 0 \ (i,j = 1,2,\ldots,n) \tag{23}$$

The 3rd equation of Eq. (23) is an auxiliary equation for conversion to an eigenproblem. Since the interlaminar stresses decay in the interior region of laminates, only the negative roots of λ^2 are selected. From the eigenproblem, $3n$ eigenvalues are obtained, and the homogeneous solutions are obtained by a $3n$-term linear combination,

$$f_i^{(\mathrm{H})} = v_{ij}^f t_j e^{-\lambda_j \xi}$$

$$p_i^{(\mathrm{H})} = v_{ij}^p t_j e^{-\lambda_j \xi} \quad (i = 1,2,\ldots,n), \ (j = 1,2,\ldots,3n), \tag{24}$$

where t_j are constants to be determined from the boundary conditions.

The particular solutions can be obtained from the assumption that $f_i(\xi)$ and $p_i(\xi)$ in Eq. (19) are constants,

$$a_{ij}^{(0)} f_j^{(\mathrm{P})} + b_{ij}^{(0)} p_j^{(\mathrm{P})} = -r_i$$

$$b_{ij}^{(0)} f_j^{(\mathrm{P})} + c_{ij}^{(0)} p_j^{(\mathrm{P})} = -s_i \quad (i,j = 1,2,\ldots,n). \tag{25}$$

Accordingly, the in-plane stress functions are expressed as the sum of the homogeneous and particular solutions,

$$f_i = f_i^{(\mathrm{H})} + f_i^{(\mathrm{P})}$$

$$p_i = p_i^{(\mathrm{H})} + p_i^{(\mathrm{P})} \quad (i = 1,2,\ldots,n). \tag{26}$$

Calculation of t_j completes the determination of the in-plane functions. The coefficients t_j can be determined from the zero boundary conditions of σ_2, σ_4 and σ_6 at the free edge,

$$v_{ij}^f t_j = -f_i^{(\mathrm{P})},$$

$$\lambda_j v_{ij}^f t_j = 0$$

$$v_{ij}^p t_j = -p_i^{(\mathrm{P})} \quad (i = 1,2,\ldots,n),\ (j = 1,2,\ldots,3n). \tag{27}$$

Substituting the calculated in-plane stress functions into Eq. (9), the interlaminar stresses for Case II are given as follows. The interlaminar stresses for Case I can be obtained by substituting h_i and h_i^{I} for g_i^{I} and g_i^{II}.

$$\sigma_2 = \left[v_{ij}^f t_j e^{-\lambda_j \xi} + f_i^{(\mathrm{P})}\right] g_i^{\mathrm{II}}(\eta),$$

$$\sigma_3 = \lambda_j^2 v_{ij}^f t_j e^{-\lambda_j \xi} g_i(\eta),$$

$$\sigma_4 = \lambda_j v_{ij}^f t_j e^{-\lambda_j \xi} g_i^{\mathrm{I}}(\eta),$$

$$\sigma_5 = \lambda_j v_{ij}^p t_j e^{-\lambda_j \xi} h_i(\eta)$$

$$\sigma_6 = \left[v_{ij}^p t_j e^{-\lambda_j \xi} + p_i^{(\mathrm{P})}\right] h_i^{\mathrm{I}}(\eta) \quad (i = 1,2,\ldots,n),\ (j = 1,2,\ldots,3n). \tag{28}$$

2.2. 2nd process: improvement of out-of-plane stress functions

The 1st process provides accurate prediction of interlaminar stresses [Fig. 2(a)] along the in-plane direction, but it produces undesirable oscillations in the out-of-plane direction [Fig. 2(b)]. The CLT solutions cannot be recovered in the interior region (Fig. 4). Thus, the one-step process is insufficient for the accurate prediction of the interlaminar stresses.

The extended Kantorovich method is applied to improve interlaminar stress predictions. By assuming layer-dependent out-of-plane stress functions in each layer and reapplying the principle of complementary virtual work, the out-of-plane functions can be improved.

The in-plane stress functions determined from the 1st process are substituted into the complementary energy density functions. The partial differentiations of g_i and h_i are carried out for Case I and Case II. Since g_i and h_i are defined for each layer, the compatibility equations are also obtained in terms of $g_i^{(k)}$ and $h_i^{(k)}$ for each layer.

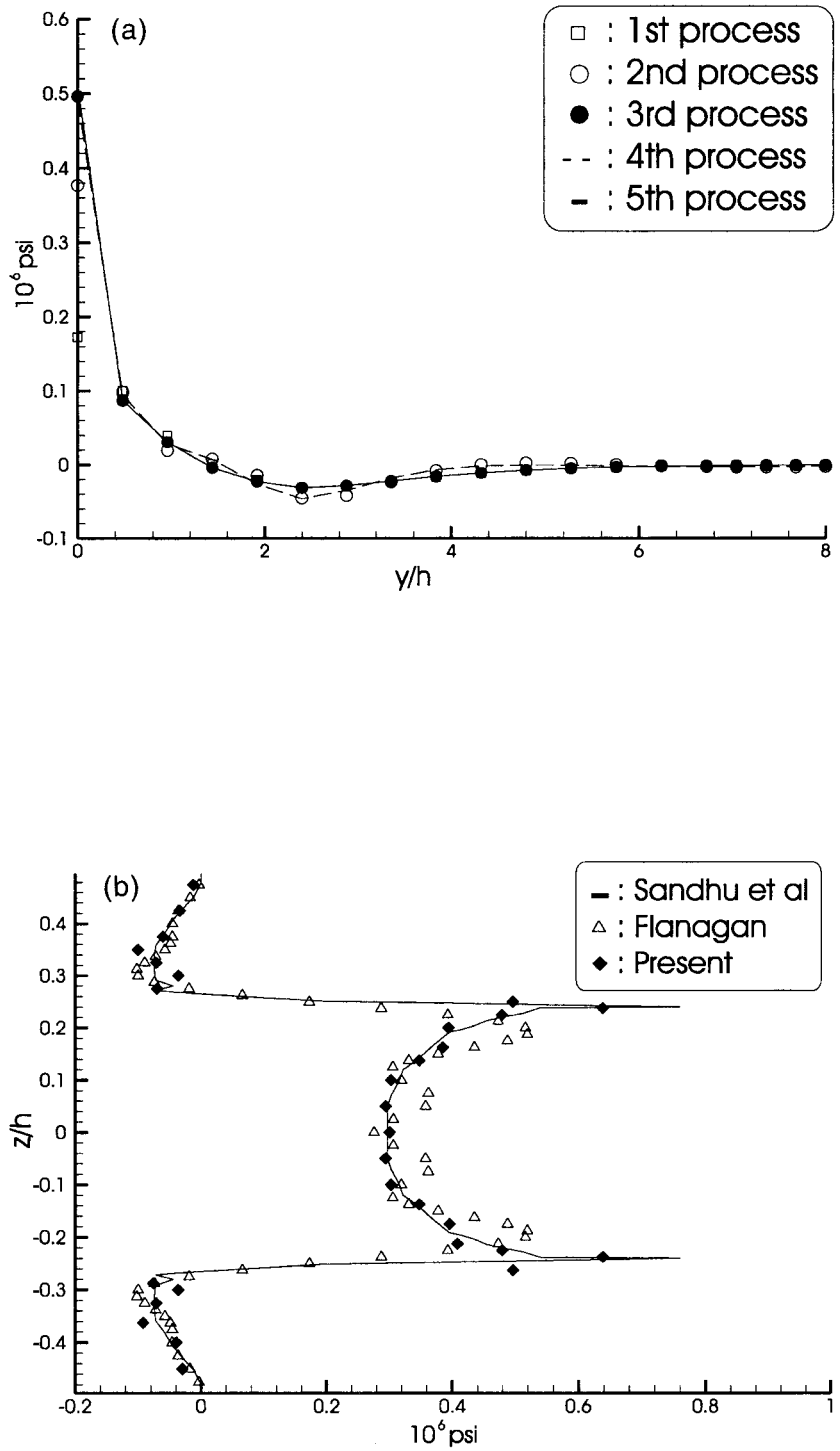

Fig. 2. (a) σ_3 at the 0/90 interface of $[0/90]_S$ laminate under unit extension. (b) σ_3 at the free edge of $[0/90]_S$ laminate under unit extension.

Case I

$$\int\Big[m_{ij}^{(4)(k)}g_j^{(k)\mathrm{IV}}+m_{ij}^{(2)(k)}g_j^{(k)\mathrm{II}}+m_{ij}^{(0)(k)}g_j^{(k)}+x_i^{(k)}\Big]\delta g_i^{(k)}\,\mathrm{d}\eta+\Lambda=0\ (k=1,2,\ldots,N),\quad (i,j=1,2,\ldots,n), \tag{29}$$

where

$$m_{ij}^{(4)(k)}=\int\Big[\hat{S}_{22}^{(k)}f_if_j+\hat{S}_{26}^{(k)}\big(f_ip_j+p_if_j\big)+\hat{S}_{66}^{(k)}p_ip_j\Big]\,\mathrm{d}\xi,$$

$$m_{ij}^{(2)(k)}=\int\Big[\hat{S}_{23}^{(k)}\Big(f_if_{\ j}^{\mathrm{II}}+f_{\ i}^{\mathrm{II}}f_j\Big)+\hat{S}_{36}^{(k)}\Big(f_{\ i}^{\mathrm{II}}p_j+p_if_{\ j}^{\mathrm{II}}\Big)-\hat{S}_{44}^{(k)}f_{\ i}^{\mathrm{I}}f_{\ j}^{\mathrm{I}}-\hat{S}_{45}\Big(f_{\ i}^{\mathrm{I}}p_j^{\mathrm{I}}+p_i^{\mathrm{I}}f_{\ j}^{\mathrm{I}}\Big)-\hat{S}_{55}^{(k)}p_i^{\mathrm{I}}p_j^{\mathrm{I}}\Big]\,\mathrm{d}\xi,$$

$$m_{ij}^{(0)(k)}=\int\hat{S}_{33}^{(k)}f_{\ i}^{\mathrm{II}}f_{\ j}^{\mathrm{II}}\,\mathrm{d}\xi$$

$$x_i^{(k)}=\int\Big[\frac{S_{13}^{(k)}}{S_{11}^{(k)}}(C-Bh\eta)+\hat{\alpha}_3\Delta T\Big]f_{\ i}^{\mathrm{II}}\,\mathrm{d}\xi. \tag{30}$$

Case II

$$\int\Big[m_{ij}^{(4)(k)}g_j^{(k)\mathrm{IV}}+m_{ij}^{(2)(k)}g_j^{(k)\mathrm{II}}+m_{ij}^{(0)(k)}g_j^{(k)}+n_{ij}^{(3)(k)}h_j^{(k)\mathrm{III}}+n_{ij}^{(1)(k)}h_j^{(k)\mathrm{I}}\Big]\delta g_i^{(k)}\,\mathrm{d}\eta$$

$$+\int\Big[m_{ij}^{(3)(k)}g_j^{(k)\mathrm{III}}+m_{ij}^{(1)(k)}g_j^{(k)\mathrm{I}}+n_{ij}^{(2)(k)}h_j^{(k)\mathrm{II}}+n_{ij}^{(0)(k)}h_j^{(k)}+x_i^{(k)}\Big]\delta h_i^{(k)}\,\mathrm{d}\eta+\Lambda=0\ (k=1,2,\ldots,N),\quad (i,j=1,2,\ldots,n), \tag{31}$$

where

$$m_{ij}^{(4)(k)}=\int\hat{S}_{22}^{(k)}f_if_j\,\mathrm{d}\xi,$$

$$m_{ij}^{(3)(k)}=-\int\hat{S}_{26}^{(k)}p_if_j\,\mathrm{d}\xi,$$

$$m_{ij}^{(2)(k)}=\int\Big[\hat{S}_{23}^{(k)}\big(f_if_{\ j}^{\mathrm{II}}+f_{\ i}^{\mathrm{II}}f_j\big)-\hat{S}_{44}^{(k)}f_{\ i}^{\mathrm{I}}f_{\ j}^{\mathrm{I}}\Big]\mathrm{d}\xi,$$

$$m_{ij}^{(1)(k)}=\int\Big[\big(\hat{S}_{45}^{(k)}p_i^{\mathrm{I}}f_{\ j}^{\mathrm{I}}-\hat{S}_{36}^{(k)}p_if_{\ j}^{\mathrm{II}}\Big]\mathrm{d}\xi,$$

$$m_{ij}^{(0)(k)} = \int \hat{S}_{33}^{(k)} f_{\ i}^{\mathrm{II}} f_{\ j}^{\mathrm{II}}\, \mathrm{d}\xi,$$

$$n_{ij}^{(3)(k)} = \int \hat{S}_{26}^{(k)} f_i p_j\, \mathrm{d}\xi,$$

$$n_{ij}^{(2)(k)} = -\int \hat{S}_{66}^{(k)} p_i p_j\, \mathrm{d}\xi,$$

$$n_{ij}^{(1)(k)} = \int \left[\hat{S}_{36}^{(k)} f_{\ i}^{\mathrm{II}} p_j - \hat{S}_{45} f_{\ i}^{\mathrm{I}} p_j^{\mathrm{I}}\right] \mathrm{d}\xi,$$

$$n_{ij}^{(0)(k)} = \int \hat{S}_{55}^{(k)} p_i^{\mathrm{I}} p_j^{\mathrm{I}}\, \mathrm{d}\xi$$

$$x_i^{(k)} = \int \left[\Theta h \xi p_i^{\mathrm{I}} - \Theta h p_i\right] \mathrm{d}\xi. \tag{32}$$

Λ represents boundary terms induced from integration by parts, and the superscript (k) refers to the kth ply in the laminate.

For arbitrary independent $\delta g^{(k)}$ and $\delta h^{(k)}$, Euler equations can be obtained from Eqs. (29) and (31). The homogeneous solutions are assumed to be the exponential functions with the eigenvalues $\mu^{(k)}$.

Case I

$$g_i^{(k)} = v_i^{g(k)} e^{\mu^{(k)}\eta}. \tag{33}$$

Case II

$$g_i^{(k)} = v_i^{g(k)} e^{\mu^{(k)}\eta}$$

$$h_i^{(k)} = v_i^{h(k)} e^{\mu^{(k)}\eta}. \tag{34}$$

Substituting Eqs. (32) and (34) into Eqs. (29) and (31), the following equations are obtained for each case.

Case I

$$m_{ij}^{(0)(k)} v_j^{g(k)} + \left(m_{ij}^{(2)(k)} + \mu^{(k)} 2 m_{ij}^{(4)(k)}\right) v_j^{g^{\mathrm{II}}(k)} = 0$$

$$\mu^{(k)} 2 v_j^{g(k)} - v_j^{g^{\mathrm{II}}(k)} = 0 \tag{35}$$

Case II

$$m_{ij}^{(0)(k)} v_j^{g(k)} + \left(m_{ij}^{(2)(k)} + \mu^{(k)2} m_{ij}^{(4)(k)}\right) v_j^{g^{\mathrm{II}}(k)} + \left(n_{ij}^{(1)(k)} + \mu^{(k)2} n_{ij}^{(3)(k)}\right) v_j^{h^{\mathrm{I}}(k)} = 0,$$

$$\left(m_{ij}^{(1)(k)} + \mu^{(k)2} m_{ij}^{(3)(k)}\right) v_j^{g^{\mathrm{II}}(k)} + \left(n_{ij}^{(0)(k)} + \mu^{(k)2} n_{ij}^{(2)(k)}\right) v_j^{h^{\mathrm{I}}(k)} = 0$$

$$\mu^{(k)2} v_j^{g(k)} - v_j^{g^{\mathrm{II}}(k)} = 0 \quad (k = 1,2,\ldots,N),\ (i,j = 1,2,\ldots,n). \tag{36}$$

The 2nd equation of Eq. (35) and the 3rd equation of Eq. (36) are used to construct formal eigenproblems. Positive and negative roots of $\mu^{(k)2}$ are chosen in this process and the homogeneous solutions are constructed from $4n$ linear combinations for Case I and $6n$ linear combinations for Case II.

Case I

$$g_i^{(k)(\mathrm{H})} = v_{ij}^{g(k)} b_j^{(k)} e^{\mu_j^{(k)}\eta} \quad (k = 1,2,\ldots,N),\ (i = 1,2,\ldots,n),\ (j = 1,2,\ldots,4n). \tag{37}$$

Case II

$$g_i^{(k)(\mathrm{H})} = v_{ij}^{g(k)} b_j^{(k)} e^{\mu_j^{(k)}\eta}$$

$$h_i^{(k)(\mathrm{H})} = v_{ij}^{h(k)} b_j^{(k)} e^{\mu_j^{(k)}\eta} \quad (k = 1,2,\ldots,N),\ (i = 1,2,\ldots,n),\ (j = 1,2,\ldots,6n), \tag{38}$$

where the $b_j^{(k)}$'s are variables to be decided from the boundary and continuity conditions. $g_j^{(k)}(\eta)$ and $h_j^{(k)}(\eta)$ are assumed to be are constant in Eqs. (29) and (31).

Case I

$$m_{ij}^{(0)(k)} g_j^{(k)(\mathrm{P})} = -x_i^{(k)}. \tag{39}$$

Case II

$$m_{ij}^{(0)(k)} g_j^{(k)(\mathrm{P})} = 0$$

$$n_{ij}^{(0)(k)} h_j^{(k)(\mathrm{P})} = -x_i^{(k)} \quad (k = 1,2,\ldots,N),\ (i,j = 1,2,\ldots,n). \tag{40}$$

The out-of-plane stress functions are given as follows:

$$g_i^{(k)} = g_i^{(k)(\mathrm{H})} + g_i^{(k)(\mathrm{P})}$$

$$h_i^{(k)} = h_i^{(k)(\mathrm{H})} + h_i^{(k)(\mathrm{P})} \quad (k = 1,2,\ldots,N),\ (i = 1,2,\ldots,n). \tag{41}$$

The variables, b_j, are determined from two conditions: Firstly, out-of-plane stress functions and their first derivatives are zero at the top and bottom surfaces. Secondly, the boundary terms caused by integration by parts in Eqs. (29) and (31) must be zero. They are the stress and variationally-consistent displacement continuity conditions at the interfaces between plies.

Accordingly, the final interlaminar stresses calculated by the 2nd process are given as follows.

Case I

$$\sigma_2 = f_i(\xi)\left[\mu_j^{(k)} 2 v_{ij}^{g(k)} b_j^{(k)} e^{\mu_j^{(k)}\eta}\right],$$

$$\sigma_3 = f_i^{\mathrm{II}}(\xi)\left[v_{ij}^{g(k)} b_j^{(k)} e^{\mu_j^{(k)}\eta} + g_i^{(k)(\mathrm{P})}\right],$$

$$\sigma_4 = -f_i^{\mathrm{I}}(\xi)\left[\mu_j^{(k)} v_{ij}^{g(k)} b_j^{(k)} e^{\mu_j^{(k)}\eta}\right],$$

$$\sigma_5 = -p_i^{\mathrm{I}}(\xi)\left[\mu_j^{(k)} v_{ij}^{g(k)} b_j^{(k)} e^{\mu_j^{(k)}\eta}\right]$$

$$\sigma_6 = p_i(\xi)\left[\mu_j^{(k)} 2 v_{ij}^{g(k)} b_j^{(k)} e^{\mu_j^{(k)}\eta}\right] \quad (i = 1,2,\ldots,n),(\ j = 1,2,\ldots,4n) \tag{42}$$

Case II

$$\sigma_2 = f_i(\xi)\left[\mu_j^{(k)} 2 v_{ij}^{g(k)} b_j^{(k)} e^{\mu_j^{(k)}\eta}\right],$$

$$\sigma_3 = f_i^{\mathrm{II}}(\xi)\left[v_{ij}^{g(k)} b_j^{(k)} e^{\mu_j^{(k)}\eta} + g_i^{(k)(\mathrm{P})}\right],$$

$$\sigma_4 = -f_i^{\mathrm{I}}(\xi)\left[\mu_j^{(k)} v_{ij}^{g(k)} b_j^{(k)} e^{\mu_j^{(k)}\eta}\right],$$

$$\sigma_5 = -p_i^{\mathrm{I}}(\xi)\left[v_{ij}^{h(k)} b_j^{(k)} e^{\mu_j^{(k)}\eta} + h_i^{(k)(\mathrm{P})}\right]$$

$$\sigma_6 = p_i(\xi)\left[\mu_j^{(k)} v_{ij}^{h(k)} b_j^{(k)} e^{\mu_j^{(k)}\eta}\right] \quad (i = 1,2,\ldots,n),\ (\ j = 1,2,\ldots,6n). \tag{43}$$

2.3. 3rd process: improvement of in-plane stress functions

The 2nd process eliminates the oscillation of the out-of-plane stress distributions [Fig. 2(b)] and recovers the CLT solutions in the interior domain (Fig. 4). However, the interlaminar stresses obtained by the 2nd process still show some oscillation in the in-plane direction as n increases [Fig. 2(a)].

The iteration process is continued to eliminate this oscillation. The 3rd iteration process is same as the 1st process, except that the out-of-plane stress functions are chosen from the 2nd process.

Further improvement of out-of-plane stress function can be obtained through processes similar to the 2nd process. In-plane stress function can be improved by a process similar to the 3rd one.

3. Numerical results

For verification, composite laminates are analyzed for various layup configurations. The material properties of a ply are given as follows.

$E_1 = 20 \times 10^6$ psi,
$E_2 = E_3 = 2.1 \times 10^6$ psi
$G_{12} = G_{13} = G_{23} = 0.85 \times 10^6$ psi
$\nu_{12} = \nu_{13} = \nu_{23} = 0.21$
$\alpha_1 = 0.22 \times 10^{-6}$ in/in/°F,
$\alpha_2 = 15.2 \times 10^{-6}$ in/in/°F

The in-plane length b is assumed to be $2h$.

The in-plane and out-of-plane stress distributions are given, respectively, and they are compared to previous results. In the figures, Flanagan's results are equivalent to those of the 1st process.

3.1. Uniaxial tension

Fig. 2(a) shows the σ_3 distribution at the 0/90 interface of a $[0/90]_S$ laminate under unit extension. The plot shows the results of various iterations. The result of the 3rd process converges, and it agrees with Flanagan's results except at the free edge. As mentioned above, the result obtained by 2nd process oscillates. The peak stress at free edge is significantly improved by the present method. The distribution of σ_3 at the free edge in a $[0/90]_S$ laminate is shown in Fig. 2(b). For comparison, Sandhu's result (Sandhu et al., 1991) is shown as well. Sandhu's result was obtained by the finite element method using 288 continuous traction elements. The new results agree with those of Sandhu, and the stress singularity at the interface is predicted well.

The distribution of σ_5 at the free edge of the $[45/-45]_S$ laminate is shown in Fig. 3. Excellent agreement between the present results and those of Wang and Choi (1982) is observed. In addition, the present method accurately predicts the maximum shear stress at the interface.

The distribution of σ_2 at the interior of a $[45/-45/0/90]_S$ laminate is shown in Fig. 4. As is shown in the figure, the present method recovers the CLT solution exactly without any oscillation whereas Flanagan's method does not accord well with the CLT solution. The computational results here are obtained by a 3-time iterations with $n = 8$.

3.2. Thermal loading

The laminates, which are subject to thermal residual stress due to the curing process, are also considered. Fig. 5(a) is the distribution of σ_3 at the centerline in a $[90/0]_S$ laminate under $\Delta T = 1$. For

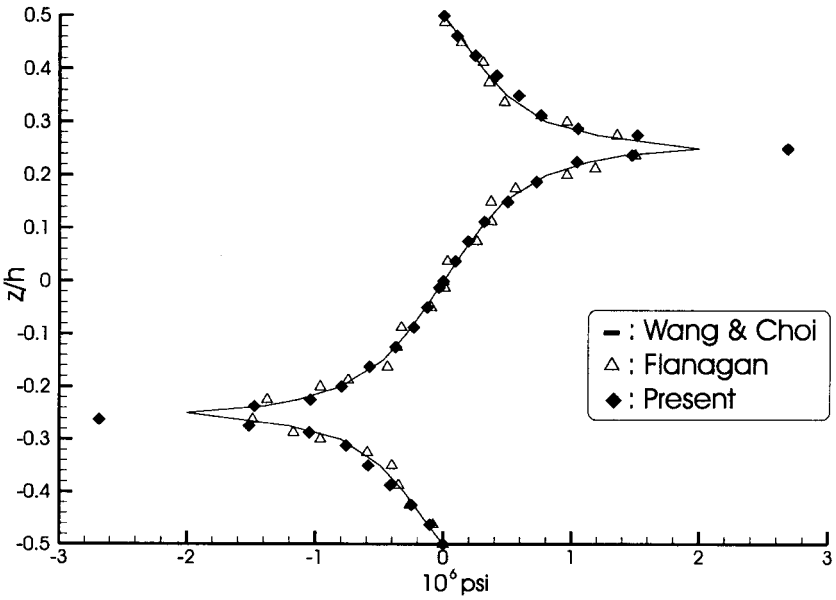

Fig. 3. σ_5 at the free edge of $[45/-45]_S$ laminate under unit extension.

comparison, Wang and Crossman (1977)'s numerical results and Kim and Atluri (1995)'s analytical results are also shown. The shape of the interlaminar stress due to thermal loading is similar to those due to extensional loading. All of the results show similar trends. The maximum stress at the free edge obtained by the present study is the largest among the three.

The distribution of σ_3 at a free edge of a $[90/0]_S$ laminate under $\Delta T = 1$ is shown in Fig. 5(b). The

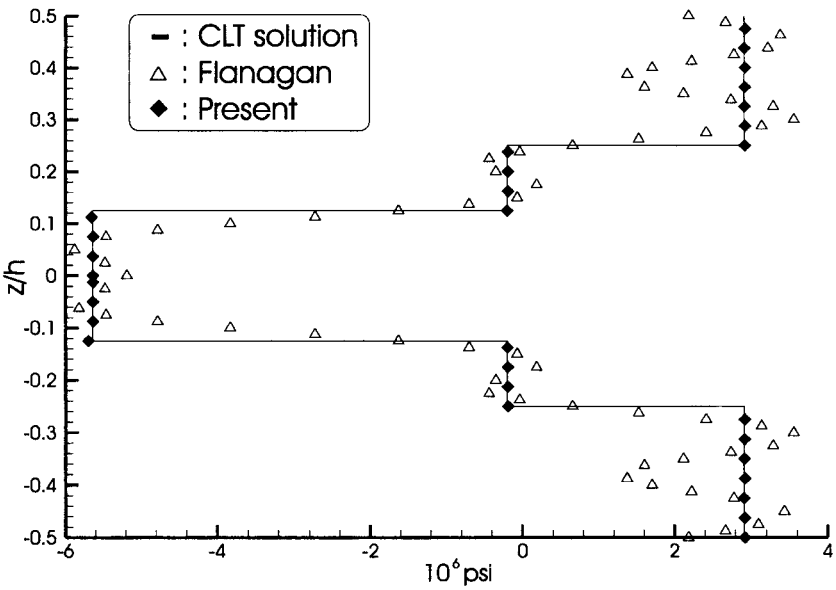

Fig. 4. σ_2 at the interior of $[45/-45/0/90]_S$ laminate under unit extension.

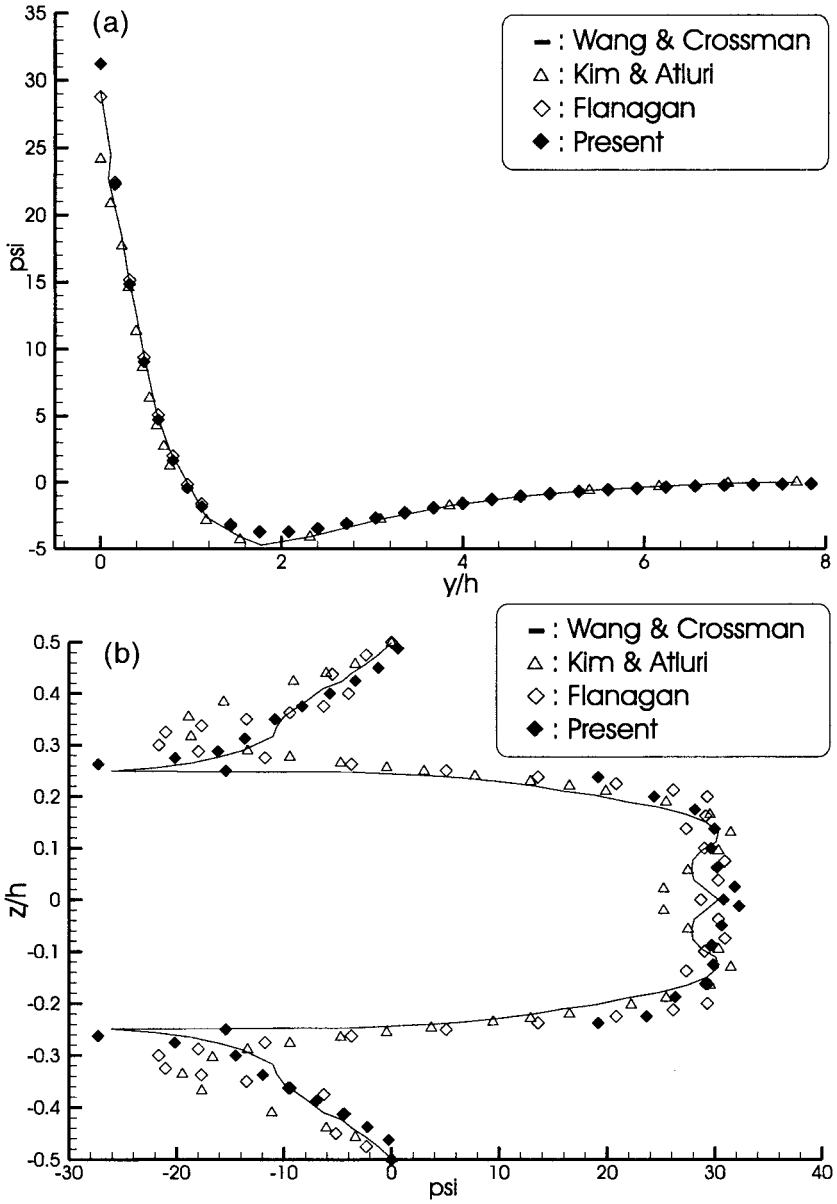

Fig. 5. (a) σ_3 at the centerline of $[90/0]_S$ laminate under $\Delta T = 1$. (b) σ_3 at the free edge of $[90/0]_S$ laminate under $\Delta T = 1$.

results of Kim and Atluri, and Flanagan do not provide accurate interlaminar stresses through the thickness. However, the results by the present method agrees well with those of Wang and Crossman. It should be emphasized that the present method correctly predicts the location and magnitude of the maximum stress accurately.

3.3. Bending

Fig. 6(a) shows σ_3 and σ_4 distributions along the in-plane direction at the 0/90 interface of a $[0/90]_s$ laminates under unit bending ($B = 1/h$). The present method provides reliable stresses which agree with those of Yin (1994a, 1994b). As the iterative process is continued, the peak stresses near the free edge becomes larger than those of Yin. Once more, the peak stress at the free edge is improved by the present iterative method. Fig. 6(b) depicts the through-the-thickness interlaminar normal stress distributions. It shows antisymmetric pattern through the thickness of the laminates. The maximum bending stress occurs at the interface between layers. The peak value is more accurately estimated through each iteration. Fig. 6(c) shows the recovery of classical lamination theory (CLT) far from the free edges. As the iterations are processed, the CLT solutions are accurately recovered in the interior domain of the laminates. Fig. 7. shows interlaminar stress distributions in the in-plane direction at the 45/−45 interface of $[45/-45]_s$ laminates. Interlaminar stresses converge well as the iteration continues. Fig. 8(a) shows interlaminar stress distribution in the in-plane direction at the 0/90 interface of $[45/-45/0/90]_s$ laminates. The peak stress increases as the iteration continues. Fig. 8(b,c) depict the distribution σ_3 and σ_5 through the thickness. They show that peak stresses occur at the interfaces.

3.4. Twisting

The distribution of σ_5 in the in-plane direction at the 0/90 interface of $[0/90]_s$ laminates, obtained by applying the computation process of Case II, is shown in Fig. 9. Since Case I cannot provide nontrivial initial interlaminar stresses in the twisting load case, the assumed base functions $h_i(\eta)$ and $g_i(\eta)$ are chosen independently. However, as the number of terms in the base function increases, numerical instability occurs. Therefore, only one-term approximation was carried out for twisting problems. Fortunately, even a one-term approximation provides convergent interlaminar stresses as the iteration continues. Iterations are processed five times to show the convergence of the calculated interlaminar stresses. However, for completeness, numerical the problems of ill-conditioned matrices should be resolved in a future study. Fig. 10(a,b) shows interlaminar stress distributions in the in-plane direction at the 45/−45 interface and σ_5 through the thickness of $[45/-45]_s$ laminates. They provide convegent peak stresses as the iteration proceeds. Fig. 10(c) depicts the recovery of interior solutions. The present iterative method demonstrates the exact recovery of CLT solutions. Fig. 11(a,c) are for $[45/-45/0/90]_s$ laminates. Once more, convergent stresses and recovery of the CLT solutions are significant.

4. Conclusions

The interlaminar stresses near free edges in composite laminates have been analyzed by the extended Kantorovich method. The calculation process requires only two iterative steps. The first step consists of a process to calculate the out-of-plane stress functions from the in-plane functions and the other, vice

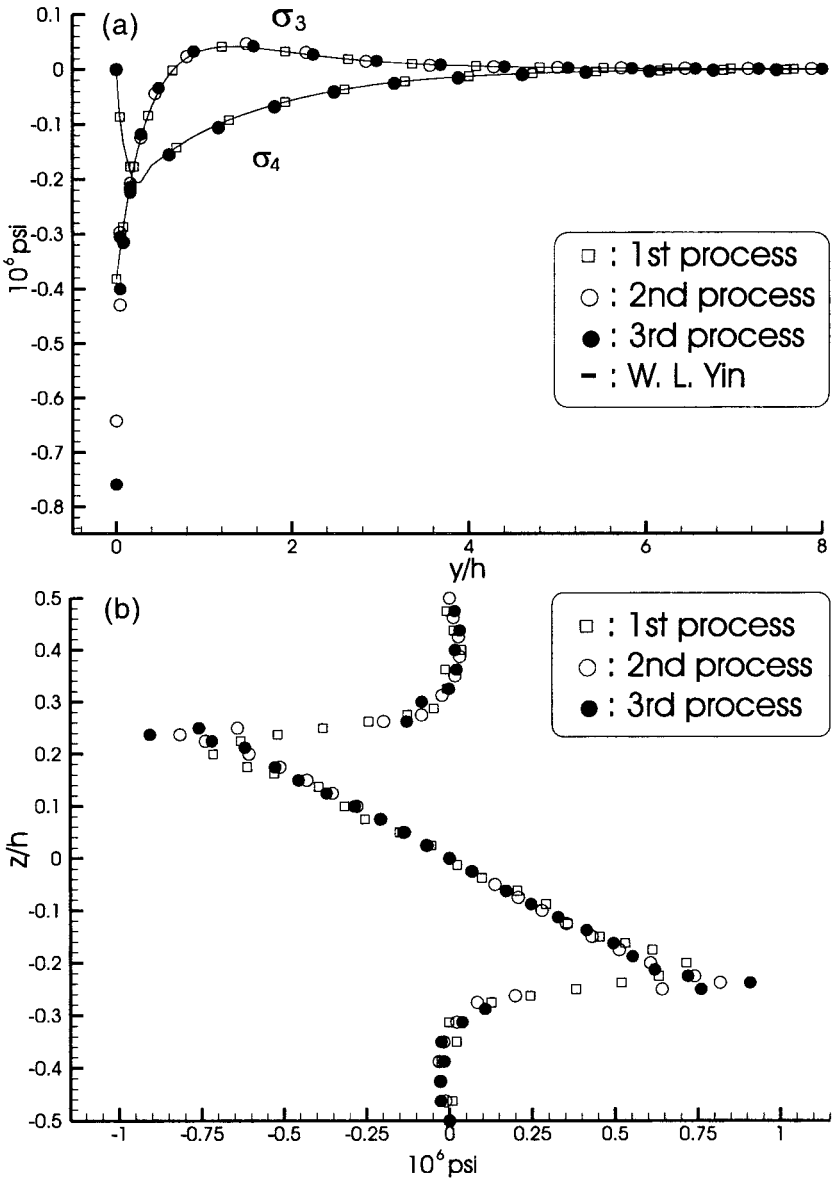

Fig. 6. (a) σ_3 and σ_4 at the 0/90 interface of $[0/90]_S$ laminate under bending ($B = 1/h$). (b) σ_3 at the free edge of $[0/90]_S$ laminate under bending ($B = 1/h$). (c) σ_2 at the interior of $[0/90]_S$ laminate under bending ($B = 1/h$).

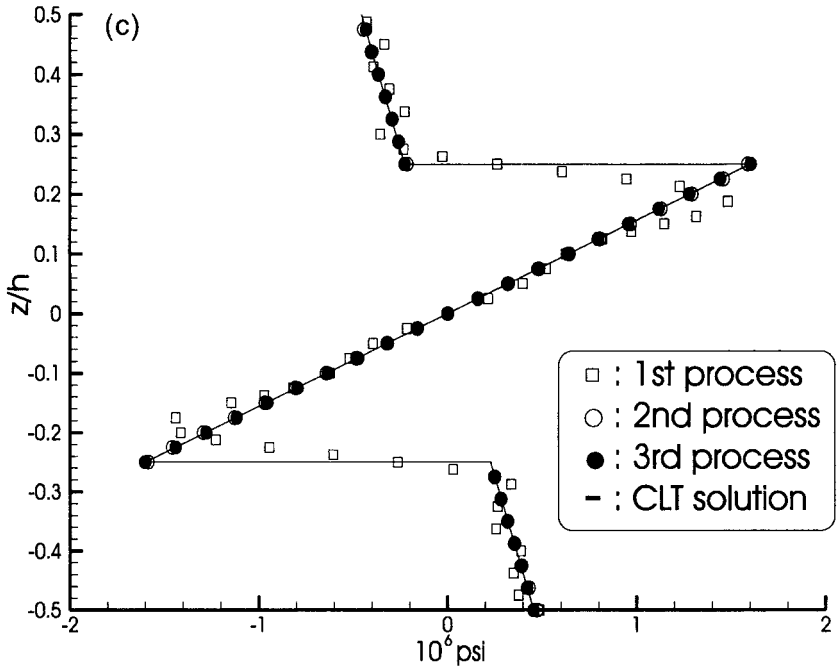

Fig. 6 (*continued.*

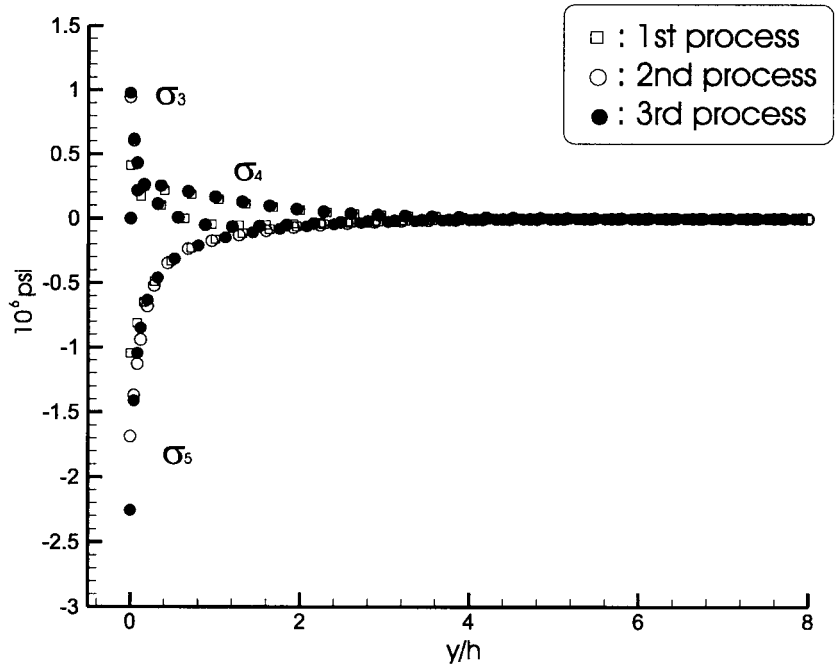

Fig. 7. σ_3, σ_4 and σ_5 at the 45/−45 interface of $[45/-45]_S$ laminate under bending ($B = 1/h$).

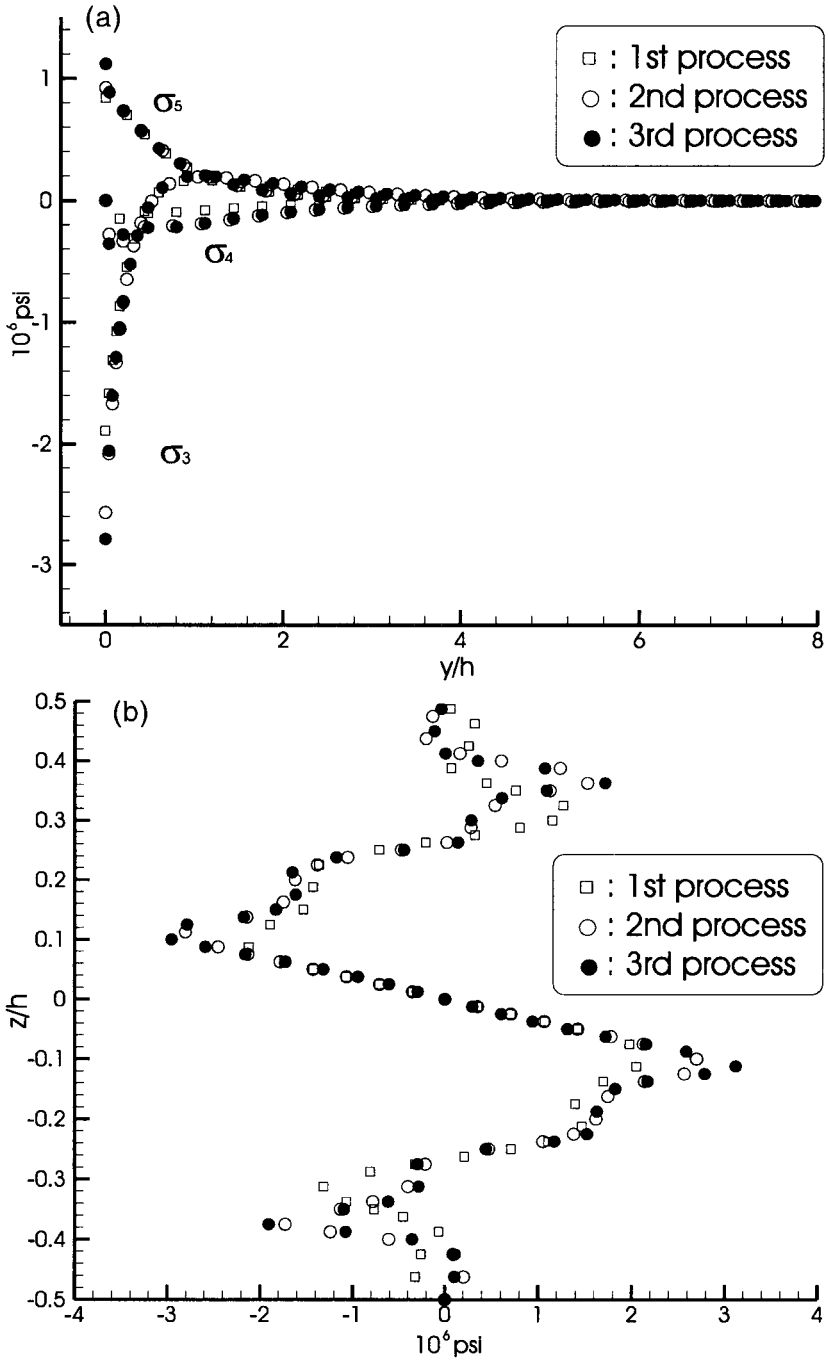

Fig. 8. (a) σ_3, σ_4 and σ_5 at the 0/90 interface of $[45/-45/0/90]_S$ laminate under bending(B = 1/h). (b) σ_3 at the free edge of $[45/-45/0/90]_S$ laminate under bending ($B = 1/h$). (c) σ_5 at the free edge of $[45/-45/0/90]_S$ laminate under bending ($B = 1/h$).

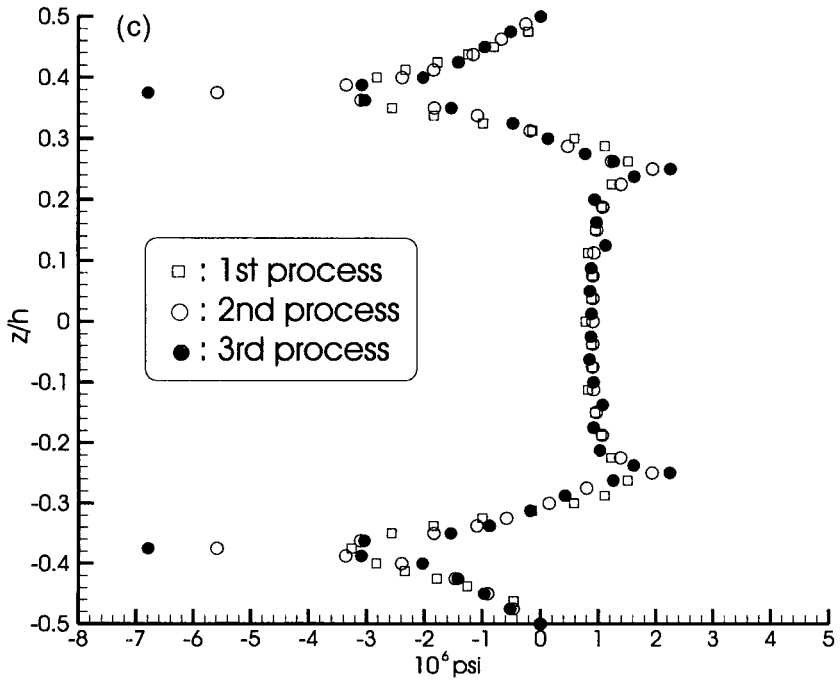

Fig. 8 (*continued*).

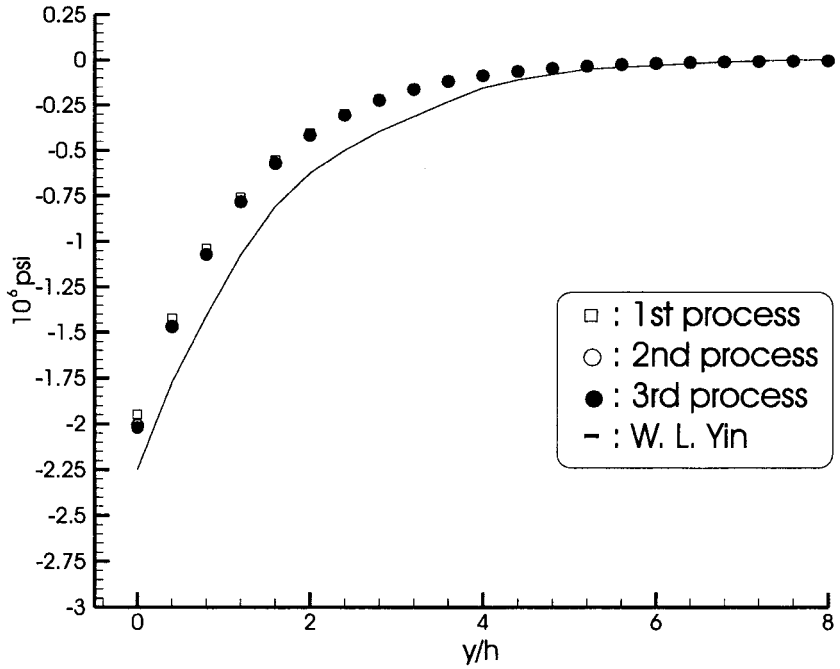

Fig. 9. σ_5 at the 0/90 interface of $[0/90]_S$ laminate under twisting ($\Theta = 1/h$).

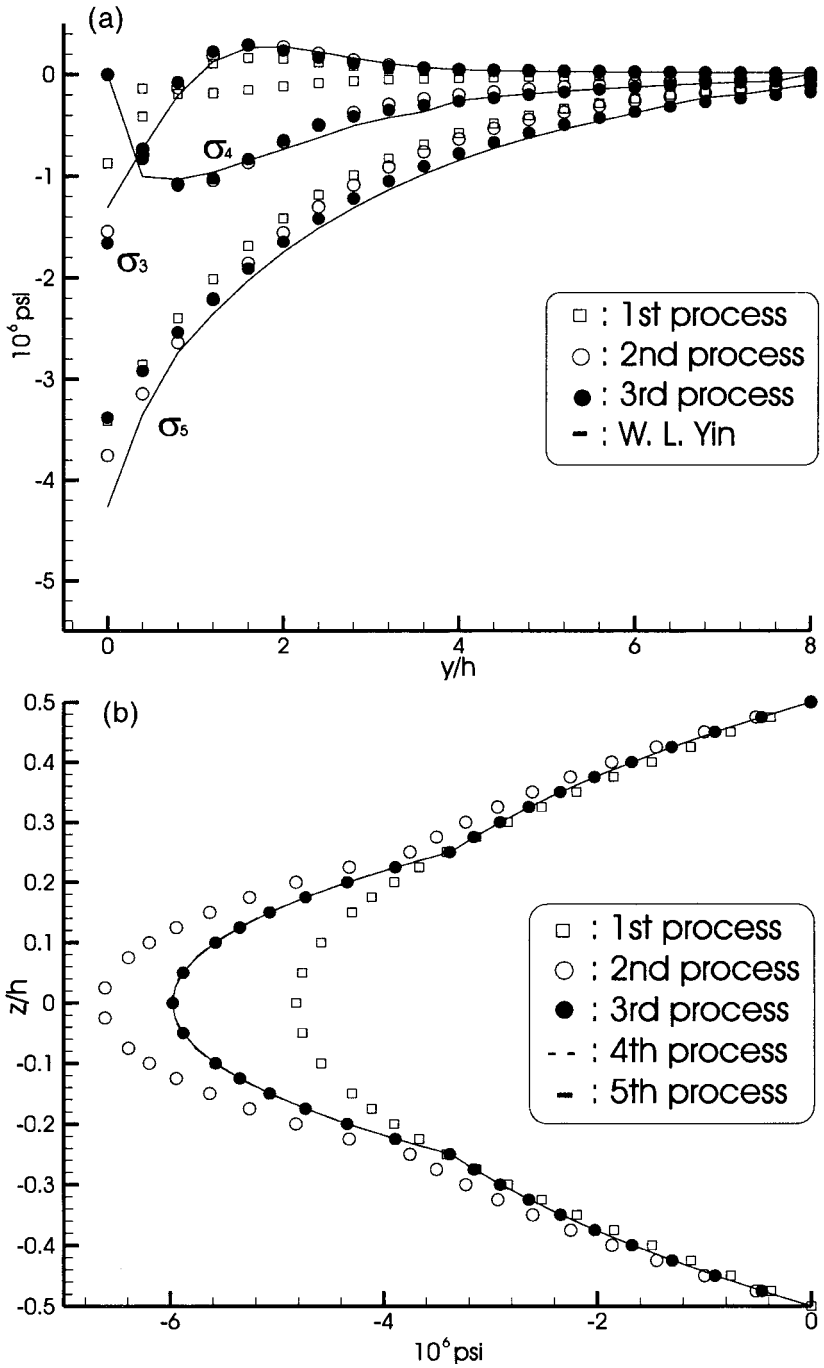

Fig. 10. (a) σ_3, σ_4 and σ_5 at the 45/−45 interface of $[45/-45]_S$ laminate under twisting ($\Theta = 1/h$). (b) σ_5 at the free edge of $[45/-45]_S$ laminate under twisting ($\Theta = 1/h$). (c) σ_2 at the interior of $[45/-45]_S$ laminate under twisting ($\Theta = 1/h$).

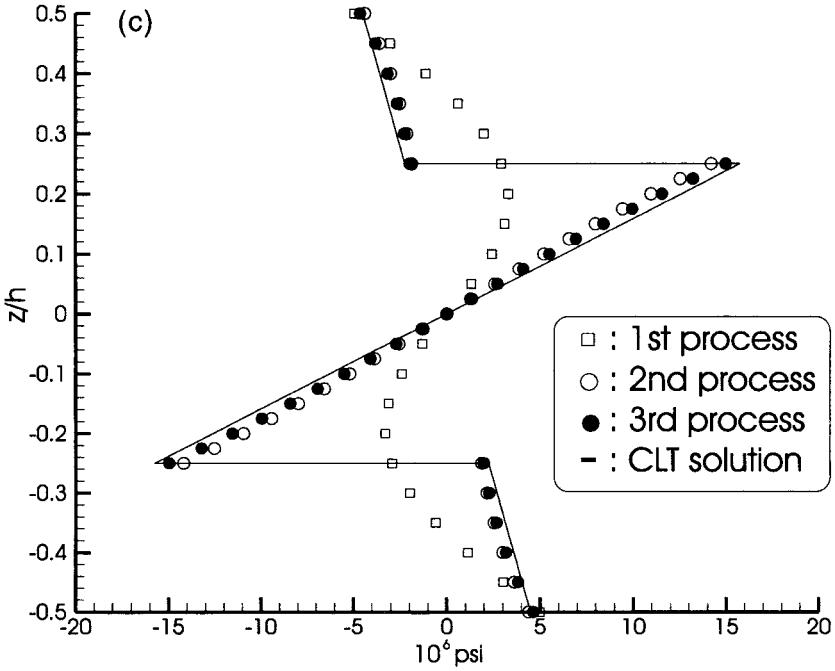

Fig. 10 (*continued*).

versa. For various symmetric layup configurations, combined mechanical loads (extension, bending and twisting) and residual thermal loads have been considered. Through the iteration process, accurate interlaminar stresses are obtained.

The results show that the high stress gradient at the free edge correlates well with the previously reported results, and the position of maximum stress was predicted accurately. The CLT solution was recovered in the interior. Therefore, the new method accurately predicts the stress distributions over the whole laminate domain.

For computational efficiency, only g_i is used as the initial base function under the extension, bending and thermal loading (Case I). However, for the twisting case (Case II), two initial base functions, g_i and h_i, are assumed independently because the base function of Case I is not sufficient to provide nontrivial solutions for twisting problems, and one-term solutions are provided in these cases. They are shown to be convergent and to recover the CLT solutions in the interior of laminates as the iteration continues.

Acknowledgements

This work was supported by the Ministry of Education, Republic of Korea, under Contract No. ME97-C-30.

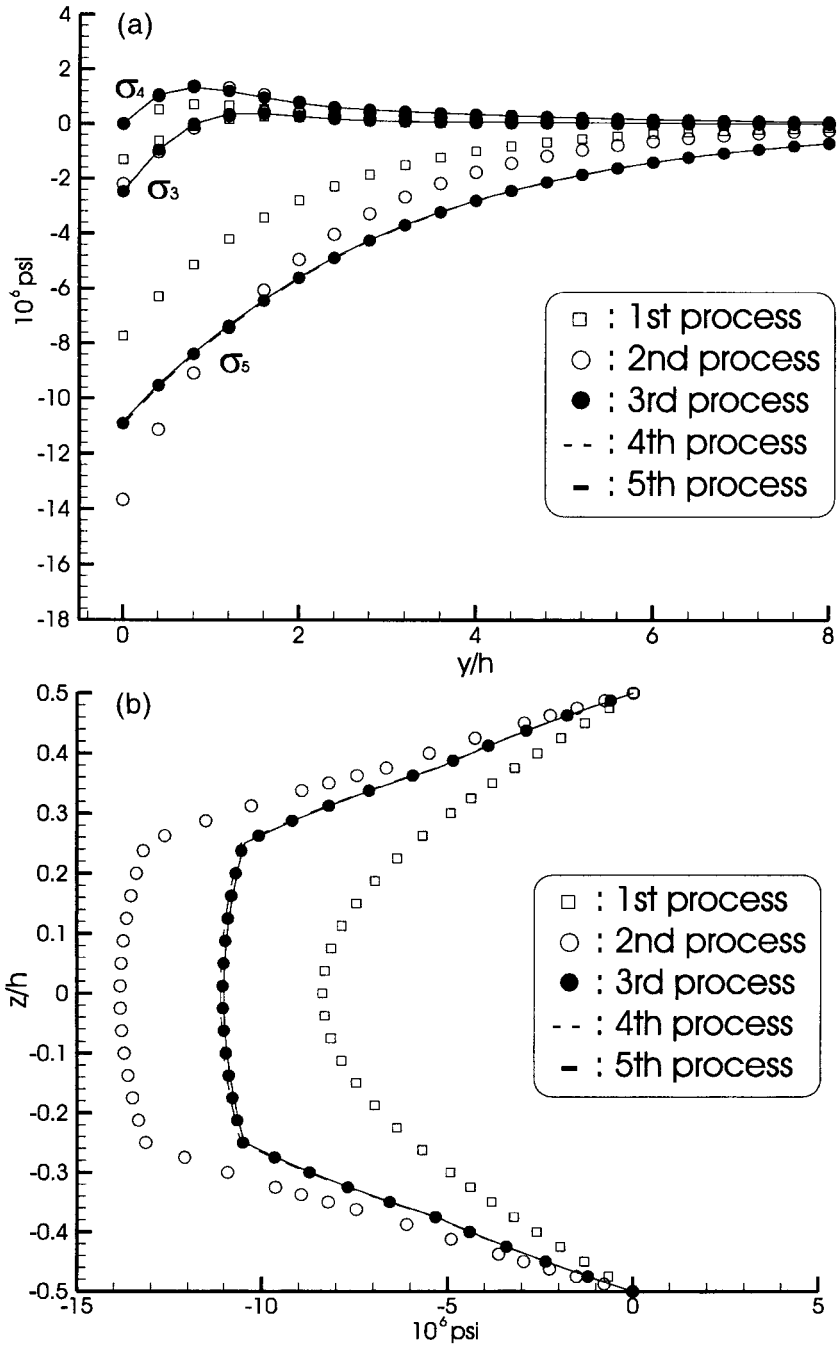

Fig. 11. (a) σ_3, σ_4 and σ_5 at the 0/90 interface of $[45/-45/0/90]_S$ laminate under twisting ($\Theta = 1/h$). (b) σ_5 at the free edge of $[45/-45/0/90]_S$ laminate under twisting ($\Theta = 1/h$). (c) σ_2 at the interior of $[45/-45/0/90]_S$ laminate under twisting ($\Theta = 1/h$).

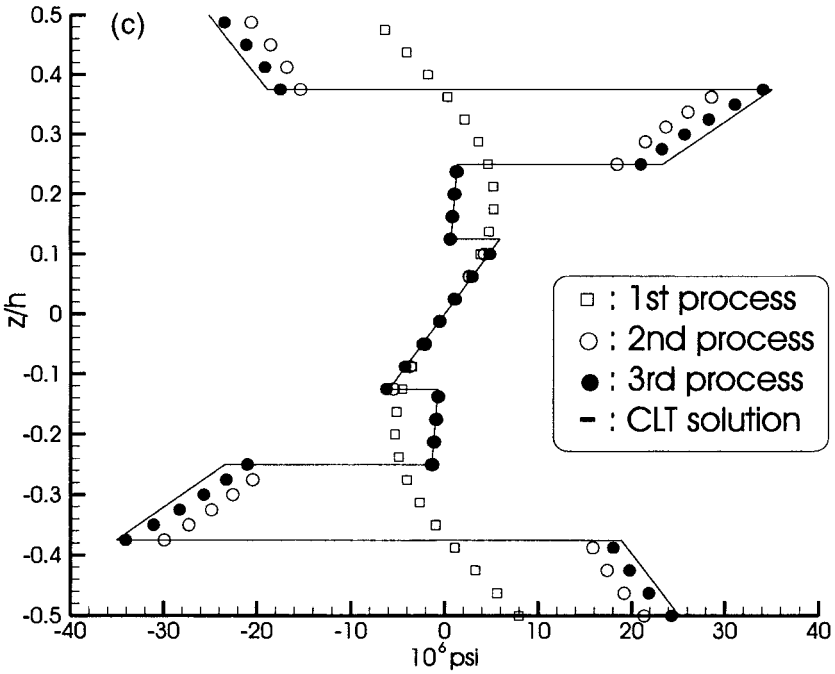

Fig. 11 (*continued*).

References

Cho, M., Yoon, J., 1997. Free-edge interlaminar stress analysis in composite laminates by the extended Kantorovich method. In: Proceedings of ICCM-11, vol. 6, pp. 648–657 Gold Coast, Australia.

Flanagan, G., 1994. An efficient stress function approximation for the free-edge stresses in laminates. International Journal of Solids and Structures 31, 941–952.

Kassapoglou, C., Lagace, P.A., 1986. An efficient method for the calculation of interlaminar stresses in composite materials. Journal of Applied Mechanics 53, 744–750.

Kim, T., Atluri, S.N., 1995. Analysis of edge stresses in composite laminates under combined thermo-mechanical loading, using a complementary energy approach. Computational Mechanics 16, 83–97.

Lekhnitskii, S.G., 1963. Theory of Elasticity of an Anisotropic Body. Holden–Day, San Francisco.

Sandhu, R.S., Wolfe, W.E., Sierakowski, R.L., Chang, C.C., Chu, H.R., 1991. Finite Element Analysis of Free-Edge Delamination in Laminated Composite Specimens U.S. Air Force Wright Laboratory Report, WL-TR-91-3022.

Spilker, R.L., Chou, S.C., 1980. Edge effects in symmetric composite laminates: importance of satisfying the traction-free-edge condition. Journal of Composite Materials 14, 2–20.

Wang, A.S.D., Crossman, F.W., 1977. Edge effects on thermally induced stresses in composite laminates. Journal of Composite Materials 11, 300–312.

Wang, S.S., Choi, I., 1982. Boundary layer effects in composite laminates: Part 2 — free edge stress solutions and basic characteristics. Journal of Applied Mechanics 49, 549–560.

Yin, W.L., 1994a. Free-edge effects in anisotropic laminates under extension, bending and twisting. Part 1 — A stress function based variational approach. Journal of Applied Mechanics 61, 410–415.

Yin, W.L., 1994b. Free-edge effects in anisotropic laminates under extension, bending and twisting. Part 2 — Eigenfunction analysis and the results for symmetric laminates. Journal of Applied Mechanics 61, 416–421.